

EDA-NOCV Analysis of Donor-Base-Stabilized Elusive Monomeric Aluminum Phosphides [(L)P-Al(L')]; L, L' = cAAC^{Me}, NHC^{Me}, PMe₃

Maria Francis and Sudipta Roy*



Cite This: ACS Omega 2022, 7, 5730–5738



Read Online

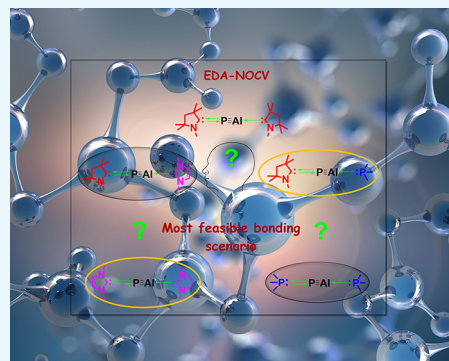
ACCESS |

Metrics & More

Article Recommendations

Supporting Information

ABSTRACT: Herein, we report on the stability and bonding analysis of donor-base-stabilized monomeric AlP species (**1–6**) of the general formula (L)P-Al(L'); [L = cAAC^{Me}, L' = cAAC^{Me}, NHC^{Me}, PMe₃, (N'Pr₂)₂ (**1–4**); L = L' = NHC^{Me}, PMe₃ (**5** and **6**); cAAC = cyclic alkyl(amino) carbene; NHC = N-heterocyclic carbene]. Energy decomposition analysis coupled with natural orbitals for chemical valence (EDA-NOCV) analysis indicates the synthetic viability of this class of species, stabilized in their singlet ground state, in the laboratory. The C_L-P bond is found to be a partial double bond (WBI ~ 1.45), while the C_L/P_L-Al bond is a single bond (WBI ~ 0.42–0.69). These bonds are mostly covalent or dative σ/π bonds depending upon the ligands attached. The central P-Al bond is an electron-sharing covalent polar single bond (WBI ~ 0.80; P-Al) for **1–4** and a dative σ bond for **5** and **6** (WBI ~ 0.89–0.93; P-Al). The calculated intrinsic interaction energies of the central P-Al bonds are found to be in the range from –116 to –216 kcal/mol (**1–3** and **5** and **6**). This value is the highest for compound **3**, possibly due to the push and pull effects from the ligands PMe₃ and cAAC, respectively.



INTRODUCTION

Having a similar outer valence shell with one crucial extra intranode in the more diffused orbitals, stabilization of multiple bonds between homo- and heterodiatomic third-row elements is of immense synthetic challenge.¹ Moreover, the weaker side-on overlap of the p-orbitals between these elements along with the significant Pauli repulsion energy keeps the synthetic chemists at the bay.² Sketching the structure of these species on the paper and subsequently trying to synthesize them in the laboratory are always intriguing.³ However, for theoretical computational chemists, it is an ambitious goal to come up with the required theoretical calculations in this technologically advanced modern world to understand and predict the stability of such species.^{3–15} In this regard, energy decomposition analysis coupled with natural orbital for chemical valence (EDA-NOCV) analysis¹⁶ is a sufficiently powerful computational tool to rationalize and predict the stability of such synthetically elusive species. Hence, EDA-NOCV is called the state-of-the-art calculation. In the past, the stability of many unusual chemical species has been predicted,¹⁷ and later on, they have been successfully synthesized by synthetic chemists and isolated in the laboratory¹⁸ in reasonable yields. In this regard, bulky ligands and/or donor-base ligands played an extremely important role. Many of such species have been stabilized by phosphines and carbenes (cAAC and NHC; cAAC = cyclic alkyl(amino) carbene, NHC = N-heterocyclic carbene) by their electronic effect rather than the steric effect.¹⁹ The synthetic success achieved by employing cAAC as a ligand in the past one and half decades²⁰ is enormous. Hence,

cAAC can be compared to a unicorn among the ligands in the field of main group chemistry in modern days.^{14,19,20} It is astonishing to take a look back at what chemists have achieved around the globe till now and yet much more to come. Many of such cAAC-containing species have now entered into the areas of application-based studies.²¹

Aluminum phosphide has attracted the attention of chemists due to its usage as a fumigant, insecticide, rodenticide, and further application as a precursor for the AlP source as composite materials in the form of a crucial intermediate in hydrogen storage.^{22–25} Very recently, the research group of H. Braunschweig isolated phospha-alumenes (**B**) with a P=Al bond utilizing a bulky aryl ligand on a P atom and a cyclopentadienyl group (Cp*) on an Al atom²⁶ after the initial prediction on the stability of the P≡Al triple bond (**A**) by the group of Ming-Der Su (Scheme 1).² In this context, it is worth mentioning a few examples of the molecular dimers and/or trimers of the P=Al species.²⁷ Fascinated by these results, we wondered whether the AlP monomer can be stabilized by introducing neutral donor-base ligands, and herein, we report on the NBO, QTAIM, and EDA-NOCV analysis of the donor-

Received: October 2, 2021

Accepted: January 27, 2022

Published: February 10, 2022



Scheme 1. Reported Monomeric Aluminum Phosphides (AlP) (**A–B**) and the Theoretically Designed Donor-Base-Stabilized Compounds (**1–6**) in the Present Study

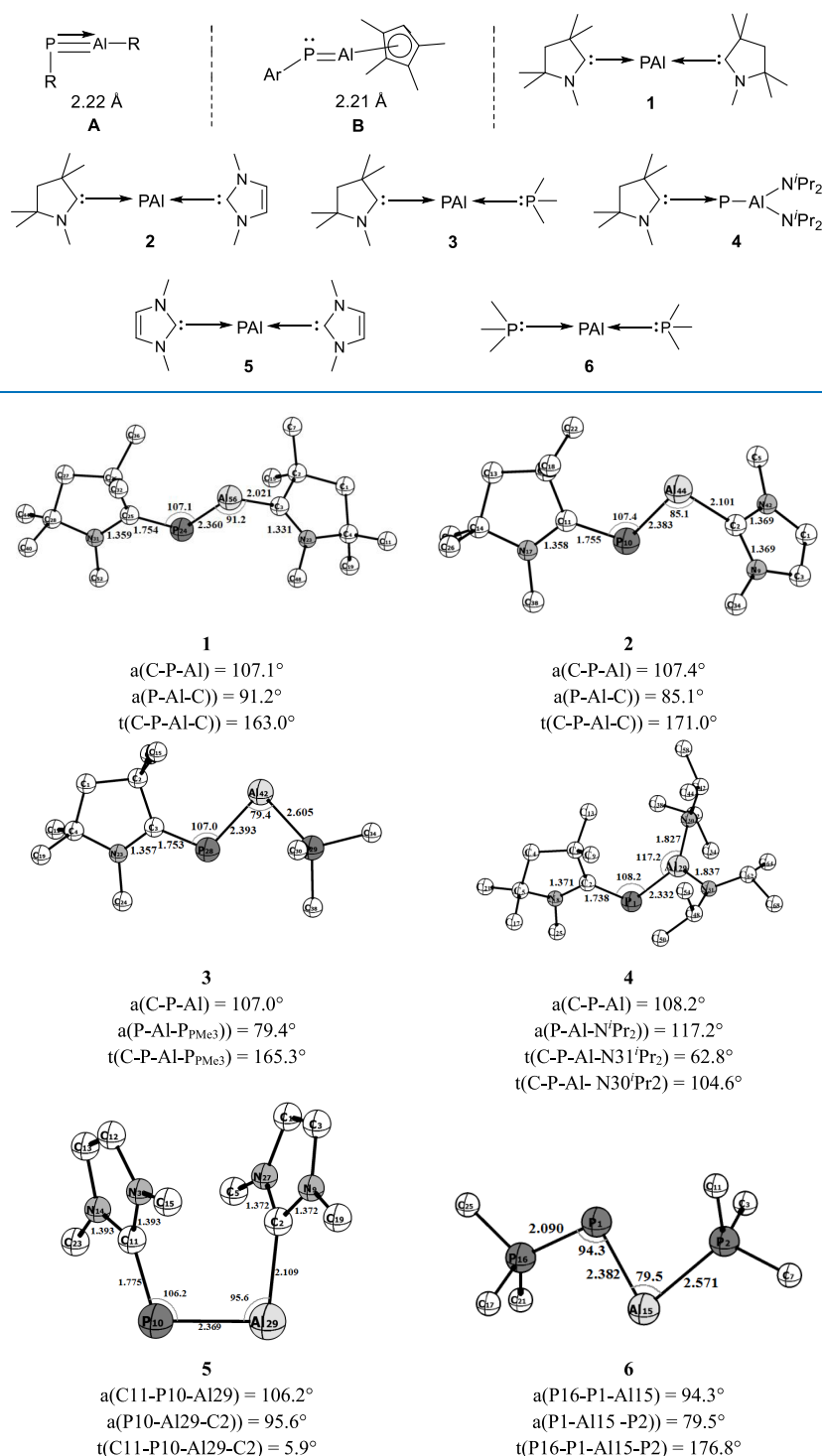


Figure 1. Optimized geometries of compounds **1–6** in the singlet ground state with $L, L' = cAAC^{Me}$ (**1**); $L = cAAC, L' = NHC^{Me}$ (**2**); $L = cAAC, L' = PMe_3$ (**3**); $L = cAAC, L' = (N^iPr_2)_2$ (**4**); $L, L' = NHC^{Me}$ (**5**); and $L, L' = PMe_3$ (**6**) at the BP86-D3(BJ)/def2-TZVPP level of theory.

base-stabilized monomeric AlP species (**1–6**) of the general formula $(L)P-Al(L')$ [$L = cAAC^{Me}, L' = cAAC^{Me}, NHC^{Me}, PMe_3, (N^iPr_2)_2$ (**1–4**); $L = L' = NHC^{Me}, PMe_3$ (**5** and **6**); $cAAC =$ cyclic alkyl(amino) carbene; $NHC = N$ -heterocyclic carbene] (Scheme 1).

COMPUTATIONAL METHODS

The geometry optimization and frequency calculations of $L-AlP-L'$ with $L, L' = cAAC^{Me}$ (cyclic alkyl(amino) carbene) (**1**), $L = cAAC^{Me}, L' = NHC^{Me}$ (*N*-heterocyclic carbene) (**2**), $L = cAAC^{Me}, L' = PMe_3$ (**3**), $L = cAAC^{Me}, L' = (N^iPr_2)_2$ (**4**), $L, L' = NHC^{Me}$ (**5**), and $L, L' = PMe_3$ (**6**) compounds **1–6** in both singlet and triplet electronic states have been performed

using the Gaussian 16 program package at the BP86-D3(BJ)/def2-TZVPP level.²⁸ The absence of imaginary frequency assured the minima of the potential energy surface (PES). The natural bond orbital (NBO)²⁹ analysis for compounds **1–6** has been performed using the NBO 6.0³⁰ program to evaluate the partial charges, Wiberg bond indices (WBI),³¹ and natural bond orbitals. EDA-NOCV analyses were performed using the ADF2020.102 program package. EDA-NOCV³² calculations were carried out at the BP86-D3(BJ)/TZ2P level using the geometries optimized at the BP86-D3(BJ)/def2-TZVPP level. The details of EDA-NOCV calculations have been given in the Supporting Information (SI).

RESULTS AND DISCUSSION

The calculations at the BP86-D3(BJ)/def2-TZVPP level suggest that compounds **1–6** are stable in their singlet ground states (Figure 1), and the corresponding triplet states are higher in energy by 8.4 (**1**)–42.20 (**4**) kcal/mol (Table S3). Despite the fact that the BP86 functional is now obsolete, we used it for the current calculations as it yielded comparable results with the experimental values both in our previous studies and also in similar studies reported in the literature.³³ In compounds **1**, **5**, and **6**, the P–Al fragment is flanked on both sides by cAAC^{Me}, NHC^{Me}, and PMe₃, whereas in compounds **2–4**, P is bound to cAAC^{Me} and Al is bound to other donor ligands like NHC^{Me} (**2**), PMe₃ (**3**), and N'Pr₂ (**4**). The variation of ligands is aimed at understanding the stability of the compounds in this study with different donor ligands. The geometries shown in Figure 1 illustrate that the ligands are arranged in *trans* fashion with respect to the P–Al moiety in **1**, **2**, **3**, and **6**, whereas in **5**, the ligands are *cis* to each other, which is also supported by their corresponding torsion angles (Figure 1). The C_{cAAC/NHC}–P bond lengths of **1–5** (Figure 1) correlate well with the recently reported theoretical/experimental values in (cAAC)₂PSi(X) and NHC-PSi(X) (X = Cl, F)^{33c} and (cAAC)P–Cl,³⁴ respectively. The Al–L bond length varies considerably depending upon the ligands employed and is the shortest in **4**, where L' is two N'Pr₂ groups, and the longest in compounds **3**, **5**, where L' is PMe₃ (Figure 1, Table S1). The Al–L' bond lengths of **2** and **4** are longer than the single bond distances found in the experimentally synthesized dimethylaluminum supported by functional amine-linked NHC ligands (1.980–1.9832 Å)³⁵ and comparable to those of [bis-NHC]Al(Br)[Fe(CO)₄] (2.048, 2.045 Å)³⁶ and [[(NHC^{Dip})(H)₂Al]₂] (2.086 Å) molecules.³⁷ The computed P–Al distances (2.33–2.57 Å) of **1–6** are longer than the reported P≡Al triple bond distance of 2.12 Å² and the P=Al double bond distance of 2.21 Å in Ar–P=Al(Cp*)²⁶, suggesting a P–Al single bond (Figure 1). The P–Al bond distances of **1–6** (Figure 1, Table S1) agree well with the P–Al single bond lengths of the Lewis base-coordinated phosphanylalumane, MesP(H)-Al(Br)(L)Bbp (2.407 Å).³⁸ The P–Al bond length (2.33 Å) in **4** is slightly shorter than the other compounds. While the cAAC–P–Al bond angle (106.2–108.2°; Figure 1, Table S2) remains almost the same in **1–5**, the P–Al–L' angle, on the other hand, varies with L' in the order of **3** (79.4°, PMe₃) < **2** (85.1°, NHC^{Me}) < **1** (91.2°, cAAC^{Me}) < **4** (117.2°, N'Pr₂) (Figure 1, Table S2). The difference in P–Al–L' angles can be attributed to the steric effect and bulkiness of the ligands (L').

We have performed NBO analysis²⁹ to understand the bonding pattern, charge distribution, and electron density

distribution. The NBO results infer that the C_{cAAC/NHC}–P bonds are similar for complexes **1–5**.

The Wiberg bond indices (WBI)³² of 1.45–1.56 (Tables 1, S4–S6) indicate the presence of a C=P double bond in

Table 1. NBO Results of the Compounds cAAC–P–Al–cAAC^{Me} (**1**), cAAC–P–Al–NHC^{Me} (**2**), and cAAC–P–Al–PMe₃ (**3**) at the BP86-D3(BJ)/def2-TZVPP Level of Theory^a

	bond	ON	polarization and hybridization (%)		WBI
compound 1	C25–P24	1.97	P: 34.2	C: 65.8	1.47
			s(19.4), p(79.8)	s(39.6), p(60.1)	
	P24–Al56	1.81	P: 78.5	Al: 21.5	0.79
compound 2	Al56–C3		s(17.5), p(81.7)	s(16.5), p(82.91)	0.69
	P10–C11	1.86	P: 61.1	C: 38.8	1.46
			s(0.1), p(99.4)	s(0.0), p(99.8)	
compound 3	1.97	P: 34.2	C: 65.8		
		s(20.0), p(79.2)	s(39.7), p(60.0)		
	P10–Al44	1.86	P: 79.2%	Al: 21.8%	0.80
compound 3	Al44–C2		s(18.3), p(80.9)	s(11.7), p(87.3)	0.53
	P28–C3	1.97	P: 34.7	C: 65.3%	1.45
		s(20.8), p(78.5)	s(39.6), p(60.1)		
compound 3	1.86	P: 61.8	C: 38.1		
		s(0.0), p(99.5)	s(0.1), p(99.8)		
	P28–Al42	1.90	P: 80.8	Al: 19.2	0.81
compound 3			s(17.3), p(81.8)	s(9.32), p(90.0)	
	Al42–P29	1.91	P: 88.9	Al: 11.7	0.42
			s(31.2), p(68.7)	S(1.1), p(94.6)	

^aOccupation number (ON), polarization, and hybridization of C_{cAAC}–P, P–Al, and Al–CL bonds.

compounds **1–4** and a partial double bond in **5** (C=P, 1.25) and **6** (P=P, 1.24), respectively. The C_{cAAC} → P σ donation arising from the overlap of sp²–sp³ hybrid orbitals is more polarized toward the ligand with an occupancy of ~1.97 e and the π back donation from P → C_{cAAC} resulting from the overlap of p-orbitals, which is more polarized toward P with an occupancy of ~1.86e (Tables 1, S4–S6), indicating a donor–acceptor interaction. The WBI values of 0.42–0.69 for the Al–C/P_L bond suggest a single bond character. In compounds **3**, **5**, and **6**, the Al–C/P_L bond is polarized toward the ligand, indicating a possible L → Al σ donation. The NBO analysis did not provide information on the occupancy and polarization of the Al–C_{cAAC} bond of compounds **1**, **2**, and **4**.

The bond order of 0.79–0.93 for the P–Al bond suggests a single bond character, which is polarized toward P since it is comparatively more polar. As expected, **4** shows two different bonding occupancies for the P–Al bond, which are polarized

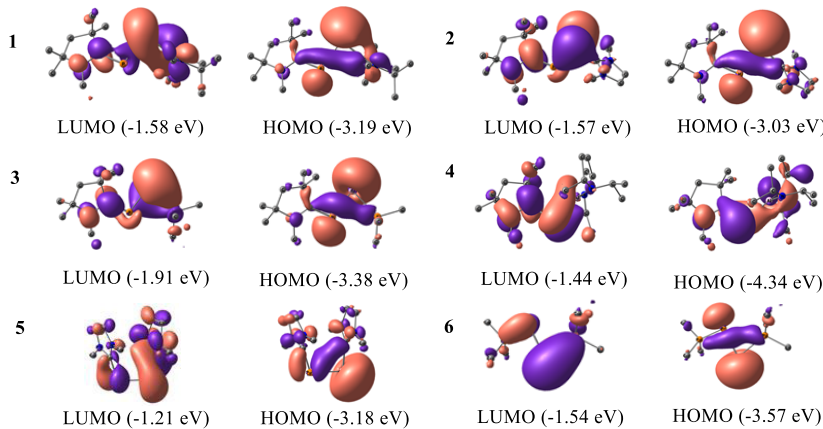
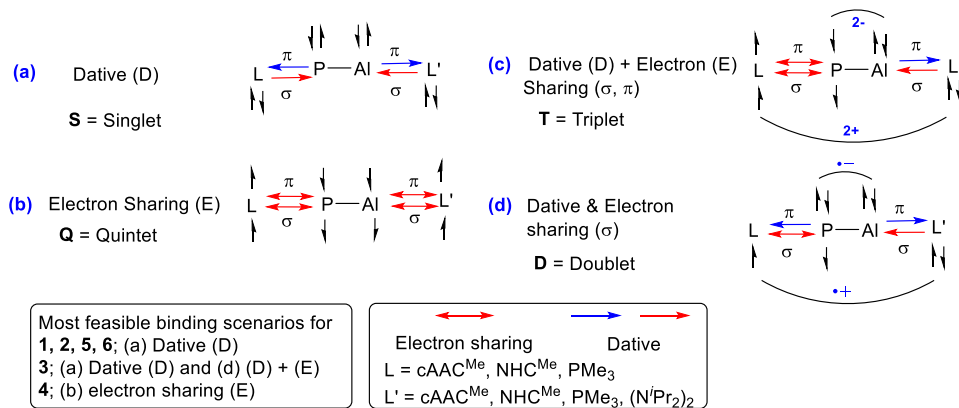


Figure 2. HOMO and LUMO of cAAC-P-Al-cAAC^{Me} (**1**), cAAC-P-Al-NHC^{Me} (**2**), cAAC-P-Al-PM₃ (**3**), cAAC-P-Al-(N*i*Pr₂)₂ (**4**), NHC^{Me}-P-Al-NHC^{Me} (**5**), and PM₃-P-Al-PM₃ (**6**) at the BP86-D3(BJ)/def2-TZVPP level of theory.

Scheme 2. Possible Bonding Scenarios of Compounds 1–6 (Also See Table S14)^a



^a(a) [L L'] and [PAI] in neutral electronic singlet states forming a dative bond, (b) [L L'] and [PAI] in neutral electronic quintet states forming four electron-sharing/covalent bonds, (c) doubly charged [L L']²⁺ and [PAI]²⁻ fragments in triplet states forming σ electron-sharing and π dative bonds, and (d) singly charged [L L']⁺ and [PAI]⁻ fragments in doublet states forming both electron-sharing and dative bonds.

toward the P atom. The highest occupied molecular orbital (HOMO) represents the lone pair of P and Al atoms in all compounds (Figure 2). In **1**, we could observe a slight interaction between the lone pair of Al atoms and cAAC with a significant coefficient residing on the Al center (Figure 2). The HOMO-1 represents the C_{cAAC}=P π bond, which is slightly extended toward Al atoms, and HOMO-2 illustrates the interaction of a lone pair on the P atom with Al (Figures S1–S6). The negative energy of the lowest unoccupied molecular orbitals (LUMOs) is attributed to the highly reactive nature of the ligands. The HOMO–LUMO energy gap ($\Delta_{\text{H-L}}$) demonstrates the electronic stability. A higher $\Delta_{\text{H-L}}$ indicates less reactivity and a lower $\Delta_{\text{H-L}}$ indicates higher reactivity. The $\Delta_{\text{H-L}}$ and thus the electronic stability of compounds vary in the following order: **2** (1.45 eV) < **3** (1.47 eV) < **1** (1.61 eV) < **5** (1.96 eV) < **6** (2.03 eV) < **4** (2.89 eV), respectively.

We investigated the topological properties of electron density ($\rho(r)$) and its Laplacian ($\nabla\rho(r)$) using quantum theory of atoms in molecules (QTAIM) analysis.³⁹ The wave functions for the QTAIM studies were computed at the BP86/def2-TZVPP level of theory on the optimized geometries of compounds **1–6**. The electron densities ($\rho(r)$) between 0.1 and 0.2,³⁹ as well as positive Laplacian ($\nabla^2\rho(r)$) at the bond critical point (BCP) of the L–P and Al–L' bonds in compounds **1–6**, indicate closed-shell interactions (Tables

S7–S12). The ellipticity, ϵ , measures the π character of the bond. When the bond is cylindrically symmetrical, as in the case of single and triple bonds, ϵ is close to zero because of the cylindrical contours of electron density. For a double bond, it is greater than zero due to the asymmetric distribution of electron density, perpendicular to the bond path.³⁹ The ϵ values of 0.157–0.308 for the C_{cAAC}=P bonds in compounds **1–4** and 0.057–0.068 (Tables S7–S12) for C_{cAAC}–P and P–P bonds in compounds **5** and **6** correlate well with the WBI values from NBO analysis and indicate a double bond character in **1–4** and a partial double character in **5** and **6**. However, unlike the NBO analysis, the ϵ values of Al–L' (0.163–0.312) also reveal a double bond character. The ϵ values for the P–Al bond, on the other hand, support the single bond character in almost all complexes except compounds **4** and **5** (Tables S7–S12).

We have employed energy decomposition analysis coupled with natural orbitals for chemical valence (EDA-NOCV)¹⁶ to study the nature of the bonds of compounds **1–6** [L, L' = cAAC^{Me} (**1**), L = cAAC, L' = NHC^{Me} (**2**), L = cAAC, L' = PM₃ (**3**), L = cAAC, L' = (N*i*Pr₂)₂ (**4**), L, L' = NHC^{Me} (**5**), L, L' = PM₃ (**6**)]. The EDA-NOCV method is more appropriate in explaining the nature of the bond, as one of the major strengths of the method is its ability to provide the best bonding model to represent the bonding situation in the

equilibrium geometry. The details of the method are given in the Supporting Information (SI). The bonding model with the lowest ΔE_{orb} is considered the best bonding representation since it involves the least change in the electronic charge of the fragments to create the electronic structure of the molecule.⁴⁰

To arrive at the best bonding description, we considered four different bonding possibilities (**Scheme 2**) for L–PAI–L' by changing the charge and multiplicity of the interacting fragments, [(L L')] and [PAI], which are (a) [L L'] and [PAI] in a neutral electronic singlet state forming a dative bond; (b) [L L'] and [PAI] in a neutral electronic quintet state forming four electron-sharing/covalent bonds; (c) doubly charged [L L']²⁺ and [PAI]²⁻ fragments in a triplet state forming a σ electron-sharing bond and π dative bonds; and (d) singly charged [L L']⁺ and [PAI]⁻ fragments in a doublet state forming both electron-sharing and dative bonds (see SI for the details of fragmentation schemes). The EDA-NOCV results consolidated in **Table S14** (see SI) indicate that the best bonding description in compounds **1**, **2**, **5**, and **6** comes from the interactions of neutral [L L'] and [PAI] fragments in the singlet state forming dative bonds (**Scheme 2a**) since it gives the lowest ΔE_{orb} . However, it is worth mentioning that the bonding in compound **2** can also be described in terms of a mixture of dative and electron-sharing bonds, as shown in **Scheme 2d**, due to the low ΔE_{orb} difference between the two bonding possibilities. Similarly, in compound **3**, the bonding can be described both in terms of a mixture of dative and electron-sharing (**Scheme 2d**) and exclusively dative bonds (**Scheme 2a**) since the orbital energies of possibility (a) match closely with that of possibility (d). On the other hand, for compound **4**, the bonding can be best discussed as electron-sharing (**Scheme 2b**). We have categorized and discussed the compounds showing similar bonding situations in **Tables 2**, **S15**, and **S16** for clarity.

The dissociation energy ($-De$) and the interaction energy (ΔE_{int}) demonstrate the strength of the bond. **Tables 2**, **S15**, and **S16** show that the L–PAI–L' bonds are relatively stronger in compound **4** (L = cAAC, L' = (N*i*Pr₂)₂) and weaker in compound **6** (L = L' = PMe₃). The difference between interaction energy (ΔE_{int}) and dissociation energy ($-De$) is termed preparative energy (ΔE_{prep}). The preparative energies originate from the distortions in the geometry of the fragments from their equilibrium structure to the geometry and electronic states in the compound. It often takes a significant amount of energy to excite the electrons of the fragments to the suitable excited energy states to make them ready for the formation of bonds. Therefore, the compounds with high ΔE_{prep} values indicate that the relaxed fragments are very different from the fragments in the molecules and hence only poorly reflect the electronic situation in the total molecule. According to the results, compound **3** (**Table S15**) show relatively higher preparative energy followed by **4** (**Table S16**) and **6** (**Table 2**). Compounds **1–3** and **5** possess slightly higher electrostatic (Coulombic) contributions, while **4** and **6** show higher orbital (covalent) contributions toward the total attractive interactions (ΔE_{int}) (**Tables 2**, **S15**, and **S16**). The contributions due to attractive dispersion interactions (ΔE_{disp}) are quite low (2.2–3.6%).

The breaking down of ΔE_{orb} into pairwise contributions brings more insight into the orbital interactions involved between the fragments, leading to the formation of the particular bonds in the present study. The calculations manifest four relevant orbital contributions, $\Delta E_{\text{orb}(1)}$ –

Table 2. EDA-NOCV Results at the BP86⁴⁰-D3(B)-TZ2P Level of L–PAI–L' Bonds of L–PAI–L' [L = L' = cAAC^{Me} (**1**); L = L' = NHC^{Me} (**2**); L = L' = PMe₃ (**6**)] using [L L'] and [P–Al] in the Electronic Singlet (S) States as Interacting Fragments^a

energy	Interaction	[cAAC] ₂ (S) + [(P–Al)] (S) (1)	[cAAC] (NHC) (S) + [(P–Al)] (S) (2)	[(NHC) ₂] (S) + [(P–Al)] (S) (5)	[(PMe ₃) ₂] (S) + [(P–Al)] (S) (6)
ΔE_{int}		-170.0	-159.7	-138.0	-116.1
ΔE_{orb}		521.1	486.8	438.8	340.4
ΔE_{PAI}		-19.1 (2.8%)	-17.4 (2.7%)	-14.1 (2.5%)	-16.4 (3.6%)
ΔE_{disp}		-344.1 (49.8%)	-321.3 (49.7%)	-287.9 (50.3%)	-211.2 (46.3%)
ΔE_{elstat}		-327.8 (47.4%)	-307.9 (47.6%)	-270.8 (47.3%)	-228.9 (50.1%)
ΔE_{orb}		-166.7 (50.9%)	-167.9 (54.5%)	-130.7 (48.3%)	-142.9 (62.4%)
$\Delta E_{\text{orb}(1)}$	L → P–Al ← L' σ donation	-28.4 (8.7%)	-51.3 (16.7%)	-65.8 (24.3%)	-38.6 (16.9%)
$\Delta E_{\text{orb}(2)}$	L → P–Al ← L' σ donation	-54.9 (16.7%)	-46.7 (15.2%)	-37.4 (13.8%)	-17.8 (7.8%)
$\Delta E_{\text{orb}(3)}$	L ← P–Al → L' π back donation	-51.9 (15.8%)	-17.2 (5.6%)	-17.8 (6.6%)	-13.9 (6.1%)
$\Delta E_{\text{orb}(4)}$	L ← P–Al → L' π back donation	-25.9 (7.8%)	-24.7 (8.0%)	18.7 (6.9%)	15.6 (6.8%)
$\Delta E_{\text{orb(test)}}$		28.3	28.9	24.2	40.2
$-De$		-141.7	-130.8	-113.8	-75.9

^aEnergies are in kcal/mol. ^bValues in the parentheses show the contribution to the total attractive interaction $\Delta E_{\text{elstat}} + \Delta E_{\text{orb}} + \Delta E_{\text{disp}}$. ^cValues in parentheses show the contribution to the total orbital interaction ΔE_{orb} .

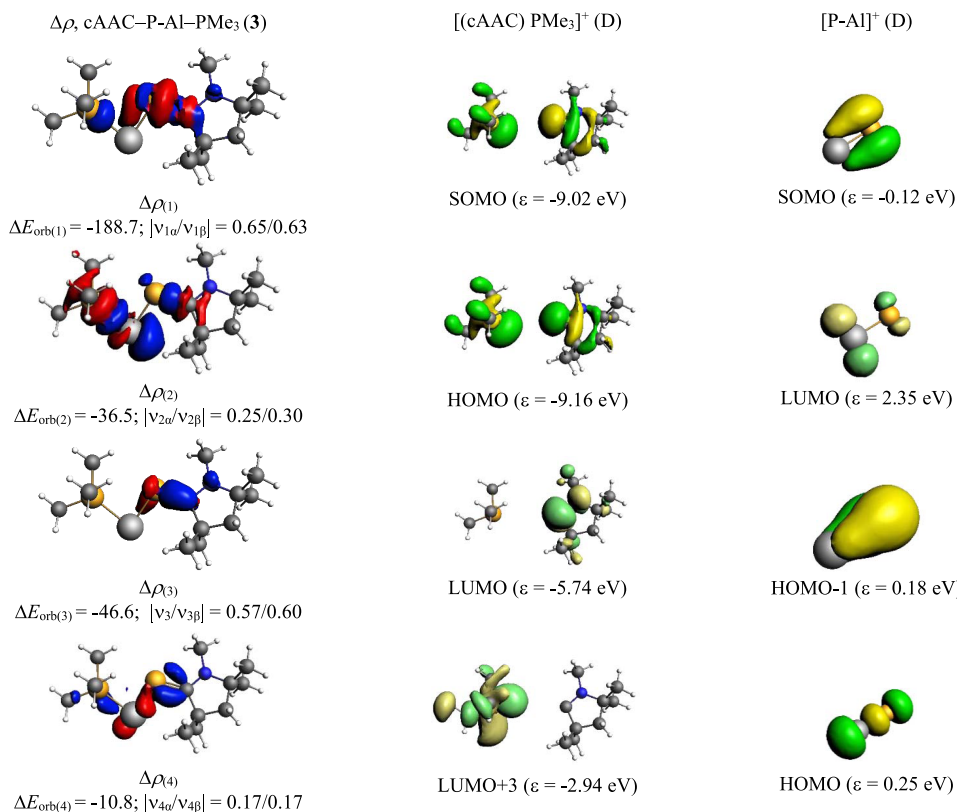


Figure 3. Shape of the deformation densities $\Delta\rho_{(1)–(4)}$ that correspond to $\Delta E_{\text{orb}(1)–(4)}$, and the associated MOs of cAAC–PAI–PMe₃ (3) and the fragments orbitals of [(cAAC) (PMe₃)]⁺ and [P–Al]⁺ in the doublet state (D) at the BP86-D3(BJ)/TZ2P level. Isosurface values are 0.003 au for $\Delta\rho_{(1)–(3)}$ and 0.001 for $\Delta\rho_{(4)}$. The eigenvalues $|\nu_n|$ give the size of the charge migration in e. The direction of the charge flow of the deformation densities is red → blue.

$\Delta E_{\text{orb}(4)}$ for compounds **1**, **2**, **5**, and **6**, which show similar bonding situations. The type of interactions and the direction of charge flow can be well understood from the deformation densities $\Delta\rho_n$ and associated fragment orbitals (Figures S17, S7, S9–10). The first two pairwise contributions $\Delta E_{\text{orb}(1)}$ and $\Delta E_{\text{orb}(2)}$ represent strong out-of-phase (+ –) σ -donation from HOMO of the ligands into the LUMO of the [PAI] fragment and rather weak in-phase (+ +) σ -donation from HOMO – 1 of the ligands into the LUMO + 1 of the [PAI] fragment, respectively, in compounds **1**, **2**, **6**. However, in compound **5**, the in-phase (+ +) σ -donation ($\Delta E_{\text{orb}(1)}$) is stronger than the out-of-phase (+ –) σ -donation ($\Delta E_{\text{orb}(2)}$). The other two pairwise contributions $\Delta E_{\text{orb}(3)}$ and $\Delta E_{\text{orb}(4)}$ denote weak π back donations from the HOMO-1 and HOMO of the [PAI] fragment into the vacant orbitals LUMO–LUMO + 4 of the ligands in compounds **1**, **2**, **5**, and **6**. The L → P–Al ← L' σ donations together contribute 59.6–79.3%, while L ← P–Al → L' π back donations together contribute 13.9–32.5% of the total orbital interactions. Compound **1** shows relatively stronger π back donations followed by **2**, **5**, and the least in compound **6**. The strength of the π back donations falls in line with the π -accepting capacity of the ligands. However, the strength of the σ donations follows the reverse order.

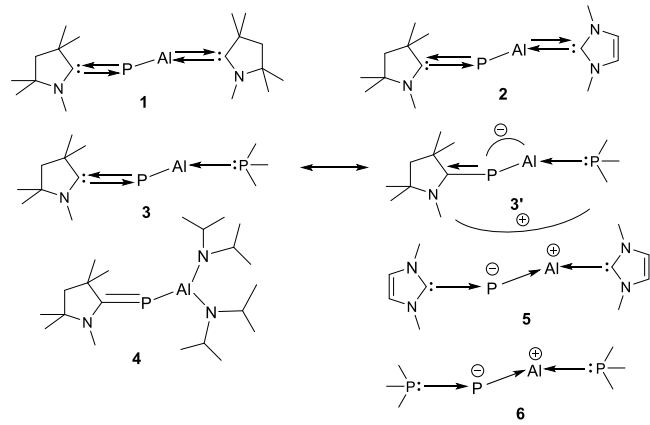
The major contribution to the ΔE_{orb} in compound **3** (Table S16) is from electron-sharing σ interaction (61.7%) occurring between the singly occupied molecular orbital (SOMO) of [(cAAC) PMe₃]⁺ and [PAI][–] ($\Delta E_{\text{orb}(1)}$). The $\Delta E_{\text{orb}(2)}$ represents in-phase σ donation (11.9%) from the [(cAAC)–(PMe₃)]⁺ fragment to the LUMO of the [PAI] fragment (Figure 3). The remaining two contributions $\Delta E_{\text{orb}(3–4)}$

indicate weak π back donations from HOMO – 1 and HOMO of the [PAI][–] fragment to the LUMO and LUMO + 3 of the [(cAAC)(PMe₃)]⁺ fragment (Figure 3), which together contributes 18.7%. The EDA-NOCV results of compound **4** reveal five important contributions to the ΔE_{orb} . The $\Delta E_{\text{orb}(1)}$ is an out-phase (+ –) σ donation from HOMO-1 of ligands [(cAAC) (NⁱPr₂)₂] into the SOMO – 1 of the [PAI] fragment with a minor contribution from SOMO – 2 of ligands (Figure S8). However, the second orbital term, $\Delta E_{\text{orb}(2)}$, arises due to the electron-sharing σ interaction between the cAAC ligand and P of the [PAI] moiety. The other two orbital terms ($\Delta E_{\text{orb}(3–4)}$) represent π electron-sharing contributions between SOMO-1, SOMO and SOMO, SOMO-3 of the interacting fragments, respectively. The last contribution is due to the out-phase dative σ donation from HOMO of the ligand fragments to the LUMO of the [PAI] fragment. It can be expressed as cAAC=P–Al(NⁱPr₂)₂. The σ interactions together contribute ~64% and π interactions together contribute 28% of the total orbital interactions. The nature of P–Al bonds of **1**–**6** has been also studied by EDA-NOCV analyses, which is schematically shown in Scheme 3 (see SI for detailed analyses).

CONCLUSIONS

We have theoretically studied the bonding and stability of monomeric AlP species by EDA-NOCV analysis, which suggests that these exotic species (**1**–**4** and **5** and **6**) are possible to stabilize and isolate in the laboratory. Ligands play an important role in their stabilizations. Both σ -donating and π -accepting properties of L and L' are in the following order: Me₃P < NⁱPr₂ < NHC < cAAC. The phosphine being a poor π

Scheme 3. Most Feasible Lewis Dot Structures of Compounds 1–4 and 5 and 6



acceptor is more suitable for an Al atom in terms of stability. The instantaneous interaction energy is computed to be lowest when L L' is PMe₃ and highest when L = cAAC and L' = NⁱPr₂. Ligands stabilize the AlP unit by σ donation and this electron-rich AlP unit gains further stability by donating back the electron densities to the adjacent ligands (\rightarrow P—Al \rightarrow) when the ligands are cAAC. This π back donation is significantly weak when donor ligands are NHC and Me₃P. Species 1–2 and 4–5 are most likely to have donor–acceptor dative bonds between AlP and ligands, while 3 can have two equally possible bonding scenarios (schemes 2 and 3). The P—Al bonds of 1–4 are electron-sharing σ bonds, while it is a σ dative P \rightarrow Al bond for 5 and 6 due to strong σ donation of NHC/Me₃P ligands.

■ ASSOCIATED CONTENT

SI Supporting Information

The Supporting Information is available free of charge at <https://pubs.acs.org/doi/10.1021/acsomega.1c05476>.

EDA-NOCV analyses and optimized coordinates of compounds 1–6 (PDF)

■ AUTHOR INFORMATION

Corresponding Author

Sudipta Roy – Department of Chemistry, Indian Institute of Science Education and Research (IISER) Tirupati, Tirupati 517507, India; orcid.org/0000-0002-5883-4329; Email: roy.sudipta@iisertirupati.ac.in

Author

Maria Francis – Department of Chemistry, Indian Institute of Science Education and Research (IISER) Tirupati, Tirupati 517507, India

Complete contact information is available at: <https://pubs.acs.org/doi/10.1021/acsomega.1c05476>

Notes

The authors declare no competing financial interest.

■ ACKNOWLEDGMENTS

M.F. thanks SMNVT Gorantla for the valuable suggestions and CSIR for the SRF. S.R. thanks SERB for the ECR grant (ECR/2016/000733) and IISER Tirupati for the financial support.

■ REFERENCES

- (1) Dasent, W. E. *Nonexistent Compounds: Compounds of Low Stability*; Marcel Dekker: New York, 1965, p 61.
- (2) Lu, J.-S.; Yang, M.-C.; Su, M.-D. Aluminum-phosphorus triple bonds: Do substituents make Al≡P synthetically accessible? *Chem. Phys. Lett.* **2017**, *686*, 60–67.
- (3) Frenking, G.; Hermann, M.; Andrada, D. M.; Holzmann, N. Donor-acceptor bonding in novel low-coordinated compounds of boron and group-14 atoms C-Sn. *Chem. Soc. Rev.* **2016**, *45*, 1129–1144.
- (4) Xiong, Y.; Yao, S.; Inoue, S.; Epping, J. D.; Driess, M. A. Cyclic Silylone (“Siladicarbene”) with an Electron-Rich Silicon(0) Atom. *Angew. Chem., Int. Ed.* **2013**, *52*, 7147–7150.
- (5) Frenking, G.; Tonner, R.; Klein, S.; Takagi, N.; Shimizu, T.; Krapp, A.; Pandey, K. K.; Parameswaran, P. New bonding modes of carbon and heavier group 14 atoms Si-Pb. *Chem. Soc. Rev.* **2014**, *43*, 5106–5139.
- (6) Niepötter, B.; Herbst-Irmer, R.; Kratzert, D.; Samuel, P. P.; Mondal, K. C.; Roesky, H. W.; Jerabek, P.; Frenking, G.; Stalke, D. Experimental Charge Density Study of a Silylone. *Angew. Chem., Int. Ed.* **2014**, *53*, 2766–2770.
- (7) Xiong, Y.; Yao, S.; Tan, G.; Inoue, S.; Driess, M. A Cyclic Germadicarbene (“Germlylone”) from Germylumylidene. *J. Am. Chem. Soc.* **2013**, *135*, 5004–5007.
- (8) Braunschweig, H.; Dewhurst, R. D.; Hammond, K.; Mies, J.; Radacki, K.; Vargas, A. Ambient-Temperature Isolation of a Compound with a Boron-Boron Triple Bond. *Science* **2012**, *336*, 1420–1422.
- (9) Wang, Y.; Xie, Y.; Wei, P.; King, R. B.; Schaefer, H. F., III; Schleyer, P. v. R.; Robinson, G. H. A Stable Silicon(0) Compound with a Si=Si Double Bond. *Science* **2008**, *321*, 1069–1071.
- (10) Sidiropoulos, A.; Jones, C.; Stasch, A.; Klein, S.; Frenking, G. N-Heterocyclic Carbene Stabilized Digermanium(0). *Angew. Chem., Int. Ed.* **2009**, *48*, 9701–9704.
- (11) Appel, R.; Schöllhorn, R. Triphenylphosphinazin [1]. *Angew. Chem.* **1964**, *76*, 991–992.
- (12) Wang, Y.; Xie, Y.; Wei, P.; King, R. B.; Schaefer, H. F., III; Schleyer, P. v. R.; Robinson, G. H. Carbene-Stabilized Diphosphorus. *J. Am. Chem. Soc.* **2008**, *130*, 14970–14971.
- (13) Abraham, M. Y.; Wang, Y.; Xie, Y.; Wei, P.; Schaefer, H. F., III; Schleyer, P. v. R.; Robinson, G. H. Carbene Stabilization of Diarsenic: From Hypervalency to Allotropy. *Chem. Eur. J.* **2010**, *16*, 432–435.
- (14) Kinjo, R.; Donnadieu, B.; Bertrand, G. Isolation of a Carbene-Stabilized Phosphorus Mononitride and Its Radical Cation (PN⁺). *Angew. Chem., Int. Ed.* **2010**, *49*, 5930–5933.
- (15) Jana, A.; Huch, V.; Rzepa, H. S.; Scheschkeiwitz, D. A Multiply Functionalized Base-Coordinated Ge^{II} Compound and Its Reversible Dimerization to the Digermene. *Angew. Chem., Int. Ed.* **2015**, *54*, 289–292.
- (16) (a) Morokuma, K. Molecular Orbital Studies of Hydrogen Bonds. III. C=O \cdots H—O Hydrogen Bond in H₂CO \cdots H₂O and H₂CO \cdots 2H₂O. *J. Chem. Phys.* **1971**, *55*, 1236–1244. (b) Ziegler, T.; Rauk, A. On the calculation of bonding energies by the Hartree Fock Slater method. *Theor. Chim. Acta* **1977**, *46*, 1–10. (c) Mitoraj, M.; Michalak, A. Donor-Acceptor Properties of Ligands from the Natural Orbitals for Chemical Valence. *Organometallics* **2007**, *26*, 6576–6580. (d) Mitoraj, M.; Michalak, A. Applications of natural orbitals for chemical valence in a description of bonding in conjugated molecules. *J. Mol. Model.* **2008**, *14*, 681–687. (e) ADF2020.102, SCM, *Theoretical Chemistry*; Vrije Universiteit: Amsterdam, The Netherlands, <http://www.scm.com>. (f) te Velde, G.; Bickelhaupt, F. M.; Baerends, E. J.; Guerra, C. F.; Gisbergen, S. J. A.; van Snijders, J. G.; Ziegler, T. Chemistry with ADF. *J. Comput. Chem.* **2001**, *22*, 931–967.
- (17) Tonner, R.; Frenking, G. C(NHC)₂: Divalent Carbon(0) Compounds with N-Heterocyclic Carbene Ligands-Theoretical Evidence for a Class of Molecules with Promising Chemical Properties. *Angew. Chem., Int. Ed.* **2007**, *46*, 8695–8698.

- (18) (a) Dyker, C. A.; Lavallo, V.; Donnadieu, B.; Bertrand, G. Synthesis of an Extremely Bent Acyclic Allene (A “Carbodicarbene”): A Strong Donor Ligand. *Angew. Chem., Int. Ed.* **2008**, *47*, 3206–3209. (b) Fürstner, A.; Alcarazo, M.; Goddard, R.; Lehmann, C. W. Coordination Chemistry of Ene-1,1-diamines and a Prototype “Carbodicarbene”. *Angew. Chem., Int. Ed.* **2008**, *47*, 3210–3214.
- (19) For overview see (a) Roy, S.; Mondal, K. C.; Roesky, H. W. Cyclic Alkyl(amino) Carbene Stabilized Complexes with Low Coordinate Metals of Enduring Nature. *Acc. Chem. Res.* **2016**, *49*, 357–369. (b) Chandra Mondal, K.; Roy, S.; Roesky, H. W. Silicon based radicals, radical ions, diradicals and diradicaloids. *Chem. Soc. Rev.* **2016**, *45*, 1080–1111. (c) Braunschweig, H.; Dewhurst, R. D.; Gessner, V. H. Transition metal borylene complexes. *Chem. Soc. Rev.* **2013**, *42*, 3197–3208. (d) Légaré, M.-A.; Pranckevicius, C.; Braunschweig, H. Metallomimetic Chemistry of Boron. *Chem. Rev.* **2019**, *119*, 8231–8261. (e) Melaimi, M.; Jazzaar, R.; Soleilhavoup, M.; Bertrand, G. Cyclic (Alkyl)(amino)carbenes (CAACs): Recent Developments. *Angew. Chem., Int. Ed.* **2017**, *56*, 10046–10068. (f) Jabłński, M. Theoretical Study of N-Heterocyclic-Carbene-ZnX₂ (X = H, Me, Et) Complexes. *Materials* **2021**, *14*, 6147–6165.
- (20) Lavallo, V.; Canac, Y.; Prasang, C.; Donnadieu, B.; Bertrand, G. Stable Cyclic (Alkyl)(Amino)Carbenes as Rigid or Flexible, Bulky, Electron-Rich Ligands for Transition-Metal Catalysts: A Quaternary Carbon Atom Makes the Difference. *Angew. Chem., Int. Ed.* **2005**, *44*, 5705–5709.
- (21) Pichon, D.; Soleilhavoup, M.; Morvan, J.; Junor, G. P.; Vives, T.; Crévisy, C.; Lavallo, V.; Campagne, J.-M.; Mauduit, M.; Zazzar, R.; et al. The debut of chiral cyclic (alkyl)(amino)carbenes (CAACs) in enantioselective catalysis. *Chem. Sci.* **2019**, *10*, 7807–7811.
- (22) Behera, C.; Krishna, K.; Bhardwaj, D. N.; Rautji, R.; Kumar, A. A Case of Accidental Fatal Aluminum Phosphide Poisoning Involving Humans and Dogs. *J. Forensic Sci.* **2015**, *60*, 818–821.
- (23) Andrews, P. C.; Raston, C. L.; Roberts, B. A. Stabilised (H₂)Al-E(H)R species, E = P or As, R = C(SiMe₃)₂-(6-Me-2-pyridyl). *Chem. Commun.* **2000**, *19*, 1961–1962.
- (24) Marder, T. B. Will We Soon Be Fueling our Automobiles with Ammonia-Borane? *Angew. Chem., Int. Ed.* **2007**, *46*, 8116–8118.
- (25) Langmi, H. W.; McGrady, G. S. Non-hydride systems of the main group elements as hydrogen storage materials. *Coord. Chem. Rev.* **2007**, *251*, 925–935.
- (26) Fischer, M.; Nees, S.; Kupfer, T.; Goettel, J. T.; Braunschweig, H.; Hering-Junghans, C. Isolable Phospha- and Arsalamenes. *J. Am. Chem. Soc.* **2021**, *143*, 4106–4111.
- (27) (a) Nees, S.; Fantuzzi, F.; Wellnitz, T.; Fischer, M.; Siewert, J.-E.; Goettel, J. T.; Hofmann, A.; Härtel, M.; Braunschweig, H.; Hering-Junghans, C. Cyclo-Dipnictiadlanes. *Angew. Chem., Int. Ed.* **2021**, *60*, 24318–24325. (b) Kaptein, M.; Balmer, M.; Niemeier, L.; Hänsch, C. von. Cyclic NHC-Stabilized Silylphosphinoalanes and -Gallanes. *Dalton Trans.* **2016**, *45*, 6275–6281. (c) Wehmschulte, R. J.; Power, P. P. Reactions of (H₂AlMes*)₂ (Mes* = 2,4,6-(t-Bu)₃C₆H₂) with H₂EAr (E = N, P, or As; Ar = Aryl): Characterization of the Ring Compounds (Mes*AlNPh)₂ and (Mes*AlEPPh)₃ (E = P or As). *J. Am. Chem. Soc.* **1996**, *118*, 791–797.
- (28) (a) Becke, A. D. Density-functional exchange-energy approximation with correct asymptotic behavior. *Phys. Rev. A* **1988**, *38*, 3098–3100. (b) Perdew, J. P. Density-functional approximation for the correlation energy of the inhomogeneous electron gas. *Phys. Rev. B* **1986**, *33*, 8822–8824. (c) Grimme, S.; Ehrlich, S.; Goerigk, L. Effect of the damping function in dispersion corrected density functional theory. *J. Comput. Chem.* **2011**, *32*, 1456–1465. (d) Grimme, S.; Antony, J.; Ehrlich, S.; Krieg, H. A consistent and accurate ab initio parametrization of density functional dispersion correction (DFT-D) for the 94 elements H-Pu. *J. Chem. Phys.* **2010**, *132*, 154104–154119. (e) Weigend, F.; Ahlrichs, R. Balanced basis sets of split valence, triple zeta valence and quadruple zeta valence quality for H to Rn: Design and assessment of accuracy. *Phys. Chem. Chem. Phys.* **2005**, *7*, 3297–3305. (f) Weigend, F. Accurate Coulomb-fitting basis sets for H to Rn. *Phys. Chem. Chem. Phys.* **2006**, *8*, 1057–1065. (g) Frisch, M. J. et al. *Gaussian 16*, Revision A.03; Gaussian, Inc.: Wallingford, CT, 2016.
- (29) (a) Weinhold, F.; Landis, C. R. *Valency and Bonding. A Natural Bond Orbital Donor-Acceptor Perspective*; Cambridge University Press, Cambridge, 2005. (b) Landis, C. R.; Weinhold, F. *The NBO View of Chemical Bonding in The Chemical Bond: Fundamental Aspects of Chemical Bonding*; Frenking, G.; Shaik, S., Eds.; Wiley, 2014; p 91.
- (30) Glendening, E. D.; Landis, C. R.; Weinhold, F. NBO 6.0: Natural Bond Orbital Analysis Program. *J. Comput. Chem.* **2013**, *34*, 1429–1437.
- (31) (a) ADF2020.102, SCM, *Theoretical Chemistry*; Vrije Universiteit: Amsterdam, The Netherlands, <http://www.scm.com>. (b) Frenking, G.; Bickelhaupt, F. M. *The Chemical Bond 1. Fundamental Aspects of Chemical Bonding*, chap. The EDA Perspective of Chemical Bonding, 121; Wiley-VCH: Weinheim, 2014.
- (32) Wiberg, K. B. Application of the Pople-Santry-Segal CNDO Method to the Cyclopropylcarbinyl and Cyclobutyl Cation and to Bicyclobutane. *Tetrahedron* **1968**, *24*, 1083–1096.
- (33) (a) Nag, E.; Gorantla, S. M. N. V. T.; Arumugam, S.; Kulkarni, A.; Mondal, K. C.; Roy, S. Tridentate Nickel(II)-Catalyzed Chemo-divergent C–H Functionalization and Cyclopropanation: Regioselective and Diastereoselective Access to Substituted Aromatic Heterocycles. *Org. Lett.* **2020**, *22*, 6313–6318. (b) Kumar, J.; Gorantla, N. V. T. S. M.; Roy, S.; Paesch, A. N.; Herbst-Irmer, R.; Stalke, D.; Anusha, C.; De, S.; Parameswaran, P.; Roesky, H. W.; et al. A Dicobalt Coordination Complex with a Short Cobalt–Cobalt Distance. *ChemistrySelect* **2018**, *3*, 8221–8228. (c) Gorantla, S. M. N. V. T.; Francis, M.; Roy, S.; Mondal, K. C. Bonding and Stability of Donor Ligand-Supported Heavier Analogues of Cyanogen Halides (L')PSi(X)(L). *RSC Adv.* **2021**, *11*, 6586–6603. (d) Mondal, K. C.; Dittrich, B.; Maity, B.; Koley, D.; Roesky, H. W. Cyclic Alkyl(Amino) Carbene Stabilized Biradical of Disilicontetrachloride. *J. Am. Chem. Soc.* **2014**, *136*, 9568–9571. (e) Mondal, K. C.; Dittrich, B.; Maity, B.; Koley, D.; Roesky, H. W. Cyclic Alkyl(Amino) Carbene Stabilized Biradical of Disilicontetrachloride. *J. Am. Chem. Soc.* **2014**, *136*, 9568–9571. (f) Buchner, M. R.; Pan, S.; Poggel, C.; Spang, N.; Müller, M.; Frenking, G.; Sundermeyer, J. Di-ortho-beryllated Carbobiphosphorane: A Compound with a Metal–Carbon Double Bond to an Element of the s-Block. *Organometallics* **2020**, *39*, 3224–3231.
- (34) Roy, S.; Mondal, K. C.; Kundu, S.; Li, B.; Schürmann, C. J.; Dutta, S.; Koley, D.; Herbst-Irmer, R.; Stalke, D.; Roesky, H. W. Two Structurally Characterized Conformational Isomers with Different C–P Bonds. *Chem. - Eur. J.* **2017**, *23*, 12153–12157.
- (35) Tai, C.-C.; Chang, Y.-T.; Tsai, J.-H.; Jurca, T.; Yap, G. P. A.; Ong, T.-G. Subtle Reactivities of Boron and Aluminum Complexes with Amino-Linked N-Heterocyclic Carbene Ligation. *Organometallics* **2012**, *31*, 637–643.
- (36) Tan, G.; Szilvási, T.; Inoue, S.; Blom, B.; Driess, M. An Elusive Hydridoaluminum(I) Complex for Facile C–H and C–O Bond Activation of Ethers and Access to Its Isolable Hydridogallium(I) Analogue: Syntheses, Structures, and Theoretical Studies. *J. Am. Chem. Soc.* **2014**, *136*, 9732–9742.
- (37) Bonyhady, S. J.; Collis, D.; Frenking, G.; Holzmann, N.; Jones, C.; Stasch, A. Synthesis of a Stable Adduct of Dialane(4) (Al₂H₄) via Hydrogenation of a Magnesium(I) Dimer. *Nat. Chem.* **2010**, *2*, 865–869.
- (38) Agou, T.; Ikeda, S.; Sasamori, T.; Tokitoh, N. Synthesis and Structure of Lewis Base-Coordinated Phosphanylalumenes Bearing P–H and Al–Br Moieties. *Eur. J. Inorg. Chem.* **2018**, *2018*, 1984–1987.
- (39) (a) Bader, R.F.W. *Atoms in Molecules: A Quantum Theory*; Oxford University Press: USA, 1994. (b) Bader, R. F. W. A Quantum Theory of Molecular Structure and Its Applications. *Chem. Rev.* **1991**, *91*, 893–928. (c) Bader, R. F. W. Atoms in Molecules. *Acc. Chem. Res.* **1985**, *18*, 9–15. (d) Matta, C. F.; Boyd, R. J. *The Quantum Theory of Atoms in Molecules*; WILEY-VCH, 2007.
- (40) (a) Frenking, G.; Bickelhaupt, F. M. *The Chemical Bond 1. Fundamental Aspects of Chemical Bonding*, chap. The EDA Perspective of Chemical Bonding, 121; Wiley-VCH: Weinheim, 2014. (b) Zhang,

Q.; Li, W. -L.; Xu, C. -Q.; Chen, M.; Zhou, M.; Li, J.; Andrade, D. M.; Frenking, G. Formation and Characterization of the Boron Dicarbonyl Complex $[B(CO)_2]^-$. *Angew. Chem., Int. Ed.* **2015**, *54*, 11078–11083. (c) Zhao, L.; Hermann, M.; Schwarz, W. H. E.; Frenking, G. The Lewis electron-pair bonding model: modern energy decomposition analysis. *Nat. Rev. Chem.* **2019**, *3*, 48–63. (d) Andrés, J.; Ayers, P. W.; Boto, R. A.; Carbó-Dorca, R.; Chermette, H.; Ciosłowski, J.; Contreras-García, J.; Cooper, D. L.; Frenking, G.; Gatti, C.; et al. Nine questions on energy decomposition analysis. *J. Comput. Chem.* **2019**, *40*, 2248–2283. (e) Yang, W.; Krantz, K. E.; Freeman, L. A.; Dickie, D. A.; Molino, A.; Frenking, G.; Pan, S.; Wilson, D. J. D.; Gilliard, R. J., Jr. Persistent Borafluorene Radicals. *Angew. Chem., Int. Ed.* **2020**, *59*, 3850–3854.

□ Recommended by ACS

Pyramidal Dicationic Ge(II) Complexes with Homoleptic Neutral Pnictine Coordination: A Combined Experimental and Density Functional Th...

Rhys P. King, Gillian Reid, et al.

JULY 28, 2021

INORGANIC CHEMISTRY

READ ▶

π Back-Donation from a Beryllium Dibromide Fragment at the Expense of Its σ Strength

Lewis R. Thomas-Hargreaves, Magnus R. Buchner, et al.

DECEMBER 12, 2021

INORGANIC CHEMISTRY

READ ▶

N,C,N-Coordinated Stannylenes as Ligands in Ag(I) and Au(I) Complexes

Roman Jambor, Alexander Hoffmann, et al.

MARCH 04, 2021

ORGANOMETALLICS

READ ▶

Sterically Hindered Tellurium(IV) Catecholate as a Lewis Acid

Pavel A. Petrov, Maxim N. Sokolov, et al.

JUNE 03, 2022

INORGANIC CHEMISTRY

READ ▶

[Get More Suggestions >](#)